

Experimental demonstrations of DSP-enabled flexibility, adaptability and elasticity of multi-channel >72Gb/s over 25 km IMDD transmission systems

Jin, Wei; Zhong, Zhuqiang; Jiang, Shan; He, Jiexiang; Hu, S.H.; Chang, Da; Giddings, Roger; Hong, Han; Jin, Xianqing; O'Sullivan, Maurice; Durrant, Tim; Trewern, J.; Mariani, G.; Tang, Jianming

Optics Express

DOI:

[10.1364/OE.440115](https://doi.org/10.1364/OE.440115)

Published: 30/11/2021

Publisher's PDF, also known as Version of record

[Cyswllt i'r cyhoeddiad / Link to publication](#)

Dyfyniad o'r fersiwn a gyhoeddwyd / Citation for published version (APA):

Jin, W., Zhong, Z., Jiang, S., He, J., Hu, S. H., Chang, D., Giddings, R., Hong, H., Jin, X., O'Sullivan, M., Durrant, T., Trewern, J., Mariani, G., & Tang, J. (2021). Experimental demonstrations of DSP-enabled flexibility, adaptability and elasticity of multi-channel >72Gb/s over 25 km IMDD transmission systems. *Optics Express*, 29(25), 41363-41377. <https://doi.org/10.1364/OE.440115>

Hawliau Cyffredinol / General rights

Copyright and moral rights for the publications made accessible in the public portal are retained by the authors and/or other copyright owners and it is a condition of accessing publications that users recognise and abide by the legal requirements associated with these rights.

- Users may download and print one copy of any publication from the public portal for the purpose of private study or research.
- You may not further distribute the material or use it for any profit-making activity or commercial gain
- You may freely distribute the URL identifying the publication in the public portal ?

Take down policy

If you believe that this document breaches copyright please contact us providing details, and we will remove access to the work immediately and investigate your claim.



Experimental demonstrations of DSP-enabled flexibility, adaptability and elasticity of multi-channel $>72\text{Gb/s}$ over 25 km IMDD transmission systems

W. JIN,¹ , Z. Q. ZHONG,^{1,*} , S. JIANG,¹ J. X. HE,¹ S. H. HU,¹ D. CHANG,¹ R. P. GIDDINGS,¹ , Y. H. HONG,¹ , X. Q. JIN,¹ M. O'SULLIVAN,² T. DURRANT,³ J. TREWERN,³ G. MARIANI,⁴ AND J. M. TANG¹

¹School of Computer Science and Electronic Engineering, Bangor University, Bangor, LL57 1UT, UK

²Ciena Canada, Inc., 385 Terry Fox Drive, Ottawa, Ontario K2K 0L1, Canada

³EFFECT Photonics LTD., Brixham Laboratory, Freshwater Quarry, Brixham, Devon, TQ5 8BA, UK

⁴EFFECT Photonics B.V., Kastanjelaan 400, 5617BC Eindhoven, Netherlands

*z.zhong@bangor.ac.uk

Abstract: DSP-enabled multi-channel aggregation techniques are promising for cost-effectively improving the flexibility, adaptability and elasticity of fronthaul transport networks. By utilizing orthogonal digital filtering in multi-channel aggregation in IMDD transmission systems, two DSP-enabled matching filter (MF)-free multi-channel aggregation techniques respectively based on SSB OFDM and orthogonal DSB OFDM have been reported; however, the SSB (DSB) technique has a drawback of relatively high digital filter DSP complexity (reduced adaptability to physical layer system characteristics). To effectively overcome these drawbacks associated with these two techniques, in this paper, a DSP-enabled MF-free adaptively variable SSB/DSB OFDM multi-channel aggregation technique is proposed and experimentally demonstrated, in which $>72\text{Gb/s}@25\text{ km}$ IMDD transmissions have been achieved. This work also evaluates, for the first time, the flexibility, adaptability, and elasticity of the orthogonal digital filtering-enabled multi-channel aggregation techniques. The results show that the proposed technique not only maintains the SSB technique's excellent adaptability but also possesses the DSB technique's low digital filter DSP complexity features.

© 2021 Optical Society of America under the terms of the [OSA Open Access Publishing Agreement](#)

1. Introduction

5G and beyond networks are expected to support a wide range of traffic-intensive and highly interactive applications, such as augmented reality and Internet of Things, with a large diversity of requirements in terms of bandwidth, latency, and numerology [1,2]. Mobile traffic also presents a tidal-effect characteristic with traffic load fluctuating over time and area. However, the current mobile fronthaul is mainly based on the statically configured common public radio interface (CPRI) [2,3] originally designed for point-to-point transmission and conveys digitalized orthogonal frequency division multiplexing (OFDM) in-phase and quadrature-phase (I-phase and Q-phase) waveforms with fixed data rates, independent of the actual requirements of mobile users. Such a static mobile fronthaul with dedicated, rigid and capacity-fixed connections cannot cost-effectively meet 5G and beyond requirements due to its spectral and power inefficiency. Moreover, the transport bandwidth required by the conventional CPRI-based fronthaul scales with antenna port count [4], thus greatly hindering the practical utilizations of highly desired massive multiple input multiple output (MIMO) and beamforming techniques. To alleviate the stringent bandwidth requirements of the transport network, the 3rd Generation Partnership

Project (3GPP) has proposed eight functional split options for baseband processing functionalities [4,5]. Option 7-2, Option 7-3 and Option 6 have attracted great industrial interest for fronthaul applications [5]. Different from the current CPRI-based fronthaul (corresponding to the functional split option 8) providing fixed bitrate, the functional split of Option 7-2, Option 7-3 or Option 6 enables the fronthaul to deliver variable bitrate scaling with MIMO layers [4,5]. In addition, these functional split options considerably reduce bandwidth requirements and have improved adaptability to the multi-antenna technology. As a direct result, the bandwidth demands of different radio units (RUs) connected to a distributed unit (DU) are significantly different, which are related to their corresponding actual mobile traffic load, and each RU-DU traffic exhibits the tidal-effect characteristics. To effectively cope with such complicated bandwidth demands and further fulfill 5G and beyond requirements, it is of great importance to equip fronthaul transport networks with sufficient flexibility, elasticity, adaptability, reconfigurability and compatibility to offer dynamic, fast, and ‘just-the-right-size’ DU-RU connections for significantly improving fronthaul spectral and power efficiency. This is also beneficial for effectively creating separated network slices [6] to fulfill diverse requirements of various customized applications/services and also offering tailored solutions for the network tenants as well as realizing seamless convergences of independently developed mobile networks and optical networks [7].

To support flexibility for cases where the functional splits are positioned inside base stations, the CPRI group published an enhanced CPRI (eCPRI) specification, which allows radio data transmissions via packet-based transport networks such as IP and/or Ethernet [8,9], thus leading to improved network flexibility and high statistical multiplexing gain. However, similarly to the CPRI, the eCPRI-enabled fronthaul still transmits digital data which is either bit oriented or I/Q oriented [9], thus leading to low spectral efficiency. To solve such technical challenge, transmitting analogue signals over multiple aggregated channels presents a spectrally efficient solution [10–20]. Various multi-channel aggregation and de-aggregation techniques have been reported, which can be classified into two categories: 1) radio frequency (RF)-domain channel aggregation and de-aggregation implemented by using RF components such as I/Q up-converters and RF combiner/splitter [10,11], and 2) digital signal processing (DSP)-enabled channel aggregation and de-aggregation based on, for example, fast Fourier transform (FFT) and inverse fast Fourier transform (IFFT)-enabled frequency division multiplexing (FDM) [12,13], code-division multiplexing (CDM) [14], digital up-conversion-enabled FDM [15,16], and digital shaping filter (SF) and matching filter (MF) pair-enabled digital filtering multiplexing (DFM) [17–19]. Between these two technique categories, the DSP-enabled multi-channel aggregation techniques are more cost effective, inherently flexible and reconfigurable, and more importantly, scalable to arbitrary channel counts for various bandwidth and modulation formats. However, for all of these multi-channel aggregation techniques, transmission system impairments and nonlinearity-induced channel interferences play a vital role in determining their maximum transmission performances. To mitigate the channel interferences, channel frequency guard bands [20] and/or extra DSP operations/techniques such as windowing operations [13] and cross channel interference cancellations (CCIC) [21,22] may be applied for practical implementations.

Since digital filtering provides an effective approach for minimizing multi-channel interferences, recently, a DSP-enabled MF-free single sideband (SSB) OFDM multi-channel intensity-modulation and direct-detection (IMDD) aggregation technique (MF-free SSB multi-channel technique) has been proposed [23–25], where the transmitter DSP uses digital orthogonal shaping filters to aggregate multiple gapless SSB OFDM signals without implementing the Hilbert transform operations. On the other hand, the receiver DSP employs the FFT operations to simultaneously disaggregate/demodulate the SSB OFDM signals without requiring any MFs. Point-to-point and multipoint-to-point multi-channel transmissions of the MF-free SSB multi-channel technique have been experimentally demonstrated in [24] and [25], respectively. In comparison with the SF and MF pair-enabled DFM multi-channel aggregation technique, the

MF-free SSB multi-channel aggregation technique improves the aggregated transmission capacity by a factor of ~ 1.8 and ~ 1.2 for cases of excluding and including the CCIC technique [24] respectively, this indicates that an enhanced tolerance to component/system impairments is achievable. Apart from the capacity improvements, the technique also reduces the receiver DSP complexity, for example 10-fold and 100-fold receiver DSP complexity reductions are achievable for 2 channels and >32 channels respectively [24]. Moreover, the use of the technique to realize concurrent direct end-user communications has also been experimentally demonstrated [25], which enables considerable reductions in fiber propagation delay and a $1.3\times$ enhancement of the aggregated transmission capacity, thus presenting a valuable solution for simultaneously fulfilling low latency and bandwidth requirements of 5G and beyond networks. However, for such a MF-free SSB multi-channel system with a given channel count, different channel spectral locations may result in different transmitter digital filter DSP complexities, and the lowest transmitter digital filter DSP complexity is similar to that of the SF and MF pair-enabled DFM multi-channel system.

To effectively reduce the digital filter DSP complexity at the transmitter, a DSP-enabled MF-free double sideband (DSB) OFDM multi-channel IMDD aggregation technique (MF-free DSB multi-channel technique) has been proposed [26], where multiple DSB OFDM signals each sharing a RF spectral region with another DSB OFDM signal are multiplexed by digital orthogonal filtering. The technique and the SF and MF pair-enabled DFM multi-channel aggregation technique have similar transmitter DSP procedures for channel multiplexing [26]. Therefore, the transmitter digital filter DSP complexities of these two techniques are similar which is independent of channel spectral locations. This means that the DSP complexity is potentially smaller than that in the MF-free SSB multi-channel systems for a given channel count. In the receivers, similar to the MF-free SSB multi-channel technique, a MF-free FFT operation-based DSP procedure is used to demultiplex and demodulate all the DSB signals, this ensures that the MF-free DSB multi-channel systems have relatively low receiver DSP complexity. However, the experimental results in the work show that the MF-free DSB multi-channel systems are relatively more sensitive to the channel fading effect, which is mainly attributed by chromatic dispersion [23].

Although the MF-free SSB and DSB IMDD multi-channel transmission systems present salient features, but they also have some drawbacks. In all of the previous work [23–26], only technical feasibility and transmission performances of the MF-free SSB and DSB multi-channel techniques were reported. In addition, in each of the previous work, the overall channel count was fixed to a specific value and all channels had identical channel bandwidths, uniform OFDM numerology and uniformly configured digital filters. Moreover, in [26] no experimental work was conducted. In this paper, a DSP-enabled MF-free adaptively variable SSB/DSB OFDM multi-channel IMDD aggregation technique (MF-free adaptive SSB/DSB multi-channel technique) is proposed and experimentally demonstrated, which retains the excellent features of MF-free SSB and DSB multi-channel aggregation techniques and meanwhile eliminates their drawbacks. Its DSP-enabled improvements in flexibility, adaptability and elasticity are experimentally assessed and its robustness against transmission system impairment/nonlinearity is compared with the previously reported MF-free SSB and DSB multi-channel aggregation techniques. The digital filter DSP complexities of both the present and previously published techniques are also theoretically analyzed and compared for different numbers of channels with identical/different signal lengths/traffic loads. In addition to the proposition of the new technique, the contributions of the paper also include, 1) first verifications of flexibility, adaptability, and elasticity of the MF-free orthogonal digital filtering-enabled multi-channel aggregation techniques, 2) first performance and DSP complexity comparisons of different MF-free orthogonal digital filtering-enabled aggregation multi-channel techniques, and 3) first experimental demonstrations of the feasibility of the MF-free DSB multi-channel techniques.

2. DSP-enabled flexibility, adaptability and elasticity of MF-free adaptive SSB/DSB multi-channel IMDD transmission systems

2.1. Transceiver DSP procedures

The schematic diagram of the MF-free adaptive SSB/DSB multi-channel IMDD transmission systems is illustrated in Fig. 1. As shown in this figure, the produced optical signal contains multiple gapless sub-wavelength (SW) channels, and each SW channel bandwidth can be flexibly and dynamically adjusted by transceiver DSPs. A SW channel conveys either two independent SSB OFDM bands or two independent but spectrally overlapped orthogonal DSB OFDM bands.

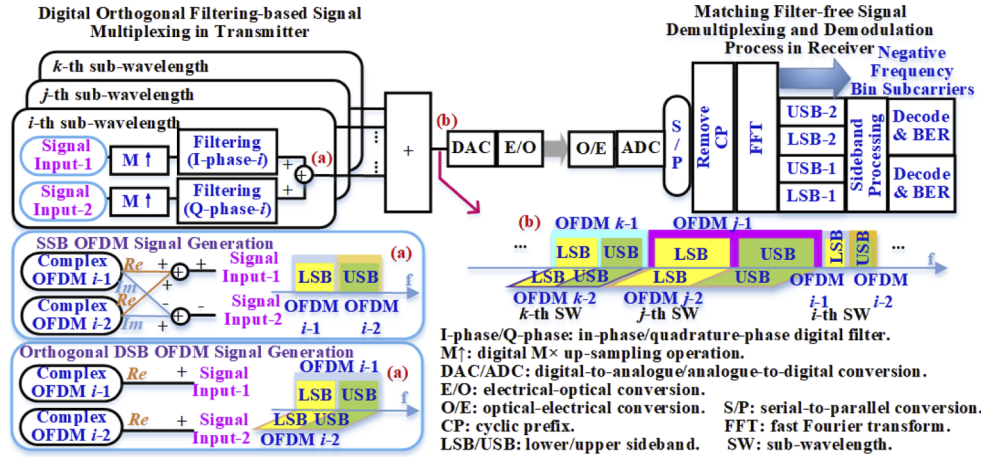


Fig. 1. Schematic diagram of MF-free adaptive SSB/DSB multi-channel IMDD transmission systems with DSP-enhanced flexibility, adaptability and elasticity.

In the transmitter, as seen in Fig. 1, complex OFDM signals are produced by setting half of the subcarriers at zeros [23]. The produced baseband OFDM signals are SSB signals. The real part and (-1) -multiplied imaginary part of each produced OFDM signal form a Hilbert transform pair, and the real part is similar to the corresponding real-valued OFDM signal produced by the Hermitian symmetry [23]. For orthogonal DSB OFDM signal generation, only the real parts of the produced complex OFDM signals undergo the following digital $M \times$ up-sampling operations ($M \uparrow$) and orthogonal digital filtering operations. The imaginary parts of the produced OFDM signals are discarded. The up-sampling operation is performed for the real parts of the produced complex OFDM signals, which is equivalent to up-sampling the corresponding real-valued OFDM signals. Therefore, after digital filtering operations, two spectrally overlapped orthogonal real-valued OFDM signals locating at the desired SW channel are produced. In IMDD systems, the MF-free DSB multi-channel technique enables the channel multiplexing operation in two physical dimensions, i.e., frequency and quadrature. While for SSB OFDM signal generations, both the real parts and the imaginary parts of the produced complex OFDM signals undergo the up-sampling operations and digital filtering operations. The digital $M \times$ up-sampling operation is performed by inserting $M-1$ zeros between adjacent samples [23], while the orthogonal digital filtering operation locates the OFDM bands at the desired SW channels [23,26]. For SSB OFDM signal generations, the DSP procedure in Fig. 1(a) allows the SSB OFDM signals to be real valued after digital filtering, and at the output, two independent SSB OFDM signals conveying different information can be produced. After the digital filtering process, all the DSB and SSB OFDM signals are combined and then converted to an analogue signal. After optical intensity modulation, the produced optical signal is fed into a fiber transmission link.

In the receiver, after optical-electrical (O-E) conversion, the analogue signal is first digitalized. In the subsequent signal demodulation process, after deleting the cyclic prefix (CP), the FFT operations are performed. For a SW channel adopting a digital up-sampling factor of M , its required FFT size is $N = M\Psi_{\text{IFFT}}$, where Ψ_{IFFT} stands for the IFFT size of the OFDM signals conveyed in the SW channel. For the SW channels requiring the same FFT size, a single FFT operation is sufficient to demodulate all the SSB/DSB OFDM signals in these SW channels. If different SW channels require different FFT sizes, multiple FFT operations each corresponding to a specific FFT size are required. Subsequently, by following the DSP procedures reported in [23], the subcarriers in each SW channel are identified after the corresponding FFT operations. For a SW channel requiring a FFT size of N , the number of subcarriers in the SW channel is Ψ_{IFFT} . To identify the subcarriers in the SW channel after the N -point FFT operation, $N/2$ subcarriers in the positive frequency bin are equally classified into $M/2$ subcarrier groups each containing Ψ_{IFFT} subcarriers. Based on the SW channel frequency location, the identifications of the subcarriers conveyed in the SW channel can be made. Because the identified Ψ_{IFFT} subcarriers are evenly distributed in the SW channel spectrum region, $\Psi_{\text{IFFT}}/2$ low frequency subcarriers and $\Psi_{\text{IFFT}}/2$ high frequency subcarriers correspond to LSB and USB signals of the SW channel. In the subsequent sideband processing, for each SW channel conveying two SSB OFDM signals, a conjugate operation and a subcarrier reverse ordering operation are applied for the LSB subcarriers, but for the USB subcarriers, no extra operations are required [23]. While for each SW channel operating at DSB, the sideband signal processing contains three DSP procedures [26], which are: 1) a conjugate operation applied only for the LSB subcarriers, 2) a pilot-aided phase recovery process for both the LSB and USB subcarriers and 3) a summation operation and a subtraction operation for the LSB and USB subcarriers. Finally, the received data are decoded after implementing the conventional OFDM equalizations.

2.2. DSP-enhanced flexibility, adaptability and elasticity as well as flexible numerology

For a SW channel adopting a digital up-sampling factor of M , its SW channel bandwidth is f_{DAC}/M [17], where f_{DAC} is the DAC sampling speed. If the SW channel conveys two orthogonal DSB OFDM bands, each DSB OFDM band has a bandwidth of f_{DAC}/M . While when conveying two SSB OFDM bands, the bandwidth of each SSB OFDM band in the same SW channel is $f_{\text{DAC}}/(2M)$. Therefore, it is easy to understand that bandwidth elasticity is achievable for each SW channel by simply varying its adopted digital up-sampling factor. On the other hand, by adaptively varying the bandwidth of each SW channel, the maximum available channel count can also be variable in a flexible and dynamic manner.

For representative IMDD transmission systems, its main transmission system impairments include the chromatic dispersion-induced channel fading effect, fiber nonlinearity, and practical hardware impairments and their interplay. The transmission impairments/nonlinearity can not only introduce channel interferences, but also lead to different subcarriers in a channel and/or in different channels suffering from signal distortions. For the MF-free DSB multi-channel techniques where the two spectrally overlapped orthogonal DSB bands in a SW channel are separated by subtracting and summing the corresponding LSB and USB subcarriers of the SW channel in the receiver, these effects also influence channel demultiplexing of spectrally overlapped signals at the receiver DSP. In a typical IMDD transmission system considered in the experimental setup subject to the strong channel fading effect, the MF-free DSB multi-channel techniques deliver relatively low transmission capacity in comparison with the MF-free SSB multi-channel techniques. This implies, compared with the MF-free SSB multi-channel system, the MF-free DSB multi-channel system is relatively sensitive to the channel fading effect. While for the SW channels suffering the minimal channel fading effect, similar aggregated transmission capacities can be delivered by both the MF-free SSB and DSB multi-channel techniques. This statement will be further verified in section 3.1. As such, in the proposed MF-free adaptive

SSB/DSB multi-channel system, the SW channels suffering the strong channel fading effect will operate at SSB to improve the signal transmission capacity, while all other SW channels will be assigned to convey DSB bands for achieving a low transmitter DSP digital filter complexity. Such adaptive SSB and DSB configuration can deliver a similar aggregated transmission capacity compared to the MF-free SSB multi-channel techniques and also a similar transmitter digital filter DSP complexity compared to the MF-free DSB multi-channel techniques. The results presented in Section 3.4 show that even for the case of $\sim 1/4$ channels operating at SSB, the proposed technique delivers a DSP complexity similar to the MF-free DSB multi-channel technique with all channels operating at DSB. Moreover, because the DSB and SSB OFDM signals have similar transceiver DSP procedures, adaptive SSB/DSB variations can also be made according to transmission system characteristics without huge transceiver DSP modifications and aggregated transmission capacity reductions.

In addition, for each SW channel, the digital filter parameters of its allocated I-phase digital filters and/or Q-phase digital filters can be adaptively reconfigured according to required bitrates. The orthogonal digital filter pairs adopted throughout this paper are constructed using a Hilbert-pair approach [27]. In comparison with the I-phase digital filters, the corresponding Q-phase digital filters have relatively lower robustness to the digital filter truncation effect [27]. Relatively long digital filter lengths are thus used for the Q-phase digital filters to achieve similar I/Q channel transmission bitrates, whilst the employment of relatively short I-phase digital filter lengths still remains to reduce the overall digital filter DSP complexity. For different SW channels, different digital filter lengths can be utilized and more importantly, their digital filter lengths can also vary adaptively according to the variations of their required transmission bitrates. Such an adaptive treatment has negligible impacts on digital filter orthogonality, this is vital for realizing digital filter-based multi-channel multiplexing.

On the other hand, due to the digital filtering process, each SW can use different OFDM parameters including CP length and subcarrier frequency spacing without introducing considerable channel interferences. This will be verified in Section 3.3. As such, for the proposed technique, flexible OFDM numerology can be applied for different SWs. 3GPP describes a numerology as a set of parameters used for configuring OFDM signals/waveforms, which include subcarrier spacing and CP overhead [28]. Different OFDM numerologies result in multiple FFT operations with different FFT sizes required in signal demodulation process as explicitly stated in Section 2.1.

2.3. DSP complexity comparisons

In this paper, the digital filter DSP complexity is defined as the total count of multiplication operations required to multiplex multiple OFDM signals. Assuming that the number of the transmitted OFDM signals is Q , for the DSB OFDM signal generation, the required digital filtering operation count is $P = Q$ [26], which is independent of channel frequency location. The digital filter DSP complexity required for multiplexing Q DSB OFDM signals is given by:

$$C_{DSB}(Q) = \sum_{i=1}^Q M_i L_i \Omega_i \quad (1)$$

where M_i and L_i stand for the up-sampling factor and the digital filter length utilized by the i -th OFDM signal, respectively. Ω_i is the signal length of the i -th OFDM signal before the up-sampling operation. To improve the spectral efficiency, transmitting Q DSB OFDM bands over $\lceil Q/2 \rceil$ SW channels is highly desirable, where $\lceil Q/2 \rceil$ rounds $Q/2$ to the nearest integer greater than or equal to $Q/2$. In this case, assuming that the numbers of the I-phase OFDM bands and the Q-phase OFDM bands are respectively $\lceil Q/2 \rceil$ and $\lfloor Q/2 \rfloor$ ($\lfloor Q/2 \rfloor$ rounds $Q/2$ to the nearest integer smaller than or equal to $Q/2$), the corresponding digital filter DSP complexity

can be expressed as,

$$C_{DSB-1}(Q) = \sum_{r=1}^{\lceil Q/2 \rceil} M_{sw-r} L_{I-r} \Omega_{I-r} + \sum_{w=1}^{\lfloor Q/2 \rfloor} M_{sw-w} L_{Q-w} \Omega_{Q-w} \quad (2)$$

where Ω_{I-r} (Ω_{Q-w}) is the signal length of the I-phase (Q-phase) OFDM band occupying the r -th (w -th) SW channel. M_{sw-r} (M_{sw-w}) is the up-sampling factor used by the r -th (w -th) SW channel. For a SW channel, the conveyed I-phase and Q-phase OFDM bands use an identical up-sampling factor. L_{I-r} (L_{Q-w}) is the I-phase (Q-phase) digital filter length used by the OFDM bands locating at the r -th (w -th) SW channel.

While for transmitting Q SSB OFDM signals, the required digital filtering operation count satisfies $2 \times \lceil Q/2 \rceil \leq P \leq 2Q$ [23]. Generally speaking, if each SSB OFDM signal does not share a SW channel with another SSB OFDM signal, the required SW channel count is Q and the required digital filtering operation count reaches its upper limit, i.e. $P=2Q$. For $P=2Q$, each OFDM signal requires 2 digital filtering operations using its allocated orthogonal digital filter pair, therefore the digital filter DSP complexity required for multiplexing Q SSB OFDM signals in Q SW channels can be expressed as:

$$C_{SSB-1}(Q) = \sum_{q=1}^Q M_{sw-q} (L_{I-q} + L_{Q-q}) \Omega_q \quad (3)$$

Comparing Eqs. (1) and (3), we can find that for the case of transmitting Q OFDM signals over Q SW channels with fixed I-phase/Q-phase digital filter lengths and constant up-sampling factors, the MF-free DSB multi-channel technique has relatively low digital filter DSP complexity in comparison with the MF-free SSB multi-channel technique. This is because that each DSB OFDM signal only utilizes a single digital filter (either an I-phase digital filter or a Q-phase digital filter) and thus requires a single digital filtering operation.

When the Q SSB OFDM signals occupy $\lceil Q/2 \rceil$ SW channels, the required digital filtering operation count reaches its lower limit, i.e. $P = 2 \times \lceil Q/2 \rceil$. For $P = 2 \times \lceil Q/2 \rceil$, the two SSB OFDM signals occupying the same SW channel share an orthogonal digital filter pair and use an identical up-sampling factor. Therefore, the corresponding digital filter DSP complexity required for multiplexing Q SSB OFDM signals in $\lceil Q/2 \rceil$ SW channels can be expressed as:

$$C_{SSB-2}(Q) = \sum_{g=1}^{\lceil Q/2 \rceil} \{M_{sw-g} (L_{I-g} + L_{Q-g}) \Omega_{g-MAX}\} \quad (4)$$

where Ω_{g-MAX} stands for the maximum signal length of the signals transmitted over the g -th SW channel. Comparing Eqs. (3) and (4), when the signal lengths, up-sampling factors and I-phase/Q-phase digital filter lengths are fixed, transmitting Q SSB signals transmitting over $\lceil Q/2 \rceil$ SW channels can not only give rise to the lowest digital filter DSP complexity but also the highest spectral efficiency.

For the proposed technique, assuming the numbers of the DSB and SSB OFDM signals are X and Y , for achieving the highest spectral efficiency, their required minimum numbers of the DSB and SSB SW channels are thus $\lceil X/2 \rceil$ and $\lceil Y/2 \rceil$. The digital filter DSP complexity can be expressed as,

$$C_{proposed}(Q) = C_{DSB-1}(X) + C_{SSB-2}(Y) \quad (5)$$

In particular, for the case of transmitting Q OFDM signals over $\lceil Q/2 \rceil$ SW channels, the digital filter DSP complexity of the proposed technique can be calculated using Eq. (6). In Eq. (6), the numbers of the SW channels operating at DSB and SSB are A and $(\lceil Q/2 \rceil - A)$, respectively. The numbers of the OFDM signals assigned for the DSB and SSB SW channels are assumed to be $2A$ and $(Q-2A)$. Such channel assignment may result in relatively high spectral efficiency because according to the operating principle of the proposed technique, the DSB SW channels suffer the

less channel fading effect than the SSB SW channels.

$$C_{proposed-1}(Q) = \sum_{r=1}^A M_{sw-r}(L_{I-r}\Omega_{I-r} + L_{Q-r}\Omega_{Q-r}) + \sum_{g=A+1}^{\lceil Q/2 \rceil} \{M_{sw-g}(L_{I-g} + L_{Q-g})\Omega_{g-MAX}\} \quad (6)$$

The first term and second term of Eq. (6) represent the digital filter DSP complexity for the DSB SW channels and the SSB SW channels, respectively. Comparing Eqs. (2), (4)-(6), for transmitting Q OFDM signals over $\lceil Q/2 \rceil$ SW channels with the fixed I-phase/Q-phase digital filter lengths and up-sampling factors, when Q is an even number and every two OFDM signals sharing the same SW channel have identical signal lengths, the MF-free DSB and SSB multi-channel techniques and the proposed technique have similar digital filter DSP complexity. The MF-free DSB multi-channel techniques can always deliver relatively low digital filter DSP complexity. For the proposed technique, when all the SW channels operate at SSB (DSB), their digital filter DSP complexity is identical to the MF-free SSB (DSB) multi-channel technique. For practical applications, due to adaptive SSB and DSB variations, as discussed in the operating principle of the proposed technique, the numbers of the SSB SW channels of the proposed technique would be smaller than the MF-free SSB multi-channel technique, thus leading to potentially low digital filter DSP complexity, in particular when the different channels have differential signal lengths or traffic loads.

When all the SW channels have identical OFDM numerology, for the proposed technique, its receiver DSP implementation complexity is slightly larger than the tradition OFDM techniques with same FFT sizes, because sideband processing requires additional operations including conjugate operation, summing/subtracting operation, subcarrier reverse ordering operation and one-tap equalizers for subcarrier phase recovery. These additional operations can be easily implemented for practical applications. Whilst for the transmitters, in comparisons with the conventional OFDM technique with an IFFT size similar to the receiver FFT size and using digital filtering operations for multi-channel aggregations, the proposed technique requires a smaller IFFT size, thus giving rise to a low DSP complexity.

3. Experimental setup and results

A point-to-point IMDD transmission system, as illustrated in Fig. 2, is utilized to experimentally investigate the feasibility, flexibility, adaptability and elasticity of the proposed technique. In the transmitter, complex OFDM signals are produced, and then up-sampled and digitally filtered following the DSP procedures depicted in Fig. 1. To produce the required orthogonal digital filters, a Hilbert-pair approach is used [27]. The OFDM signal and digital filter parameters are listed in Table 1. After the $M \times$ up-sampling operations and digital filtering process, a $1.5 \times$ digital oversampling operation and a clipping operation are applied. An AWG (Keysight M8195A) operates at 60GS/s and its output signal has a bandwidth/amplitude of 20 GHz/500mV_{pp}. A 35 GHz integrated transmitter (Thorlabs MX35D) performs optical intensity modulation, in which the differential electrical input signals first pass through an 11dB-gain RF amplifier and then drive a MZM subject to a continuous wave optical signal at ~1550.12 nm. To explore DSP-enabled channel count variation flexibility, two cases are considered here, Case I: $M1=M2=4$, where two SW channels with the same bandwidths of 10 GHz are available, and Case II: $M1=4$ and $M2=M3=8$, where three SW channels are available with the 2nd and 3rd SW channels having the same bandwidths of 5 GHz, and the 1st SW channel having a bandwidth of 10 GHz. Because each SW channel can convey two independent SSB or DSB OFDM bands, Case I can support 4 OFDM channels (CH1~CH4), whilst for Case II, 6 OFDM channels (CH1~CH6) can be transmitted. The corresponding OFDM channel spectral locations for the considered two cases are plotted in Fig. 2.

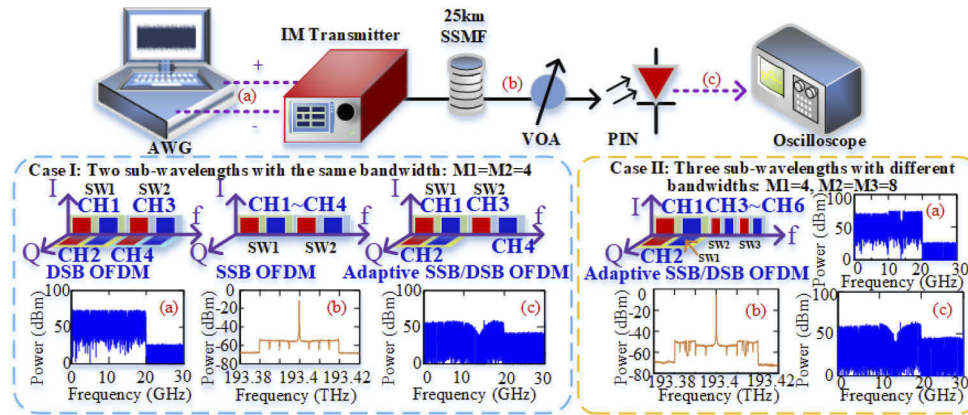


Fig. 2. Experimental setup of MF-free adaptive SSB/DSB multi-channel IMDD systems with DSP-enhanced network flexibility, adaptability and elasticity. (a) AWG output signal spectra, (b) optical signal spectra after 25 km SSMF transmission, and (c) received electrical signal spectra.

Table 1. Key Experimental Parameters

Parameter	Value
OFDM IFFT	32
Number of data-bearing subcarriers of each OFDM	15
Cyclic prefix ratio	1/16
Subcarrier modulation format	BPSK to 64-QAM
I/Q-phase digital filter length	16/32
Digital filter excess of bandwidth factor	0
Clipping Ratio	11 dB
AWG sampling speed	60GS/s
AWG output signal bandwidth/amplitude	20 GHz/500mV
Thorlabs transmitter bandwidth	35GHz
Thorlabs transmitter DFB wavelength	~1550.12nm
Thorlabs transmitter MZM half-wave voltage	~3.1V
PIN bandwidth / responsivity	40 GHz / 0.7A/W
Oscilloscope sampling speed / bandwidth	64GS/s / 40GHz
FFT size for Case I and 1 st SW of Case II	128
FFT size for 2 nd SW and 3 rd SW of Case II	256

After 25 km SSMF transmission and direct detection, a digital sampling oscilloscope (Keysight UXR0402A) digitalizes the electrical signal at a speed of 64GS/s and then sends the resulting signal to a PC for signal demodulation. The signal demodulation procedure includes signal resampling [24], frame synchronization, serial-to-parallel conversion (S/P), cyclic prefix removal, FFT operations, signal sideband identification, sideband processing, conventional OFDM subcarrier equalization and data decoding. These receiver DSP procedures are presented in Section 2.1. For these two considered cases, their required FFT sizes are listed in Table 1. For the proposed technique, the electrical signal spectra at the AWG output, the optical signal spectra after the 25 km SSMF transmission and the received electrical signal spectra at the oscilloscope input are shown in Fig. 2. For Case I, these three considered systems (SSB, DSB, and adaptive

SSB/DSB) have similar optical/electrical signal spectra. It can be found that for the experimental setup, the channel fading effect occurs at a radio frequency region of ~ 14 GHz. As such, the 2nd SW channel of Case I and the 2nd and 3rd SW channels of Case II suffer the strong channel fading effect. For both cases, the 1st SW channel suffers the negligible channel fading effect.

3.1. DSP-enhanced adaptability to physical layer system characteristics

Utilizing the experimental setup and associated parameters presented in Section 3, comparisons of measured bit error rate (BER) performances and maximum achievable signal transmission capacities are made between the proposed adaptive system and the previously reported MF-free DSB (SSB) multi-channel systems. Here only Case I is considered. With the I/Q digital filter lengths set at $L_I=16/L_Q=32$, the BER performances and signal bitrates of the four OFDM signals for these systems are respectively plotted in Fig. 3(a) and Fig. 3(b). Adaptive bit-loading is utilized in each individual OFDM signal to ensure that all the OFDM signals have similar BER performances. The aggregated signal transmission capacities of the MF-free SSB multi-channel systems, the MF-free DSB multi-channel systems and proposed MF-free adaptive SSB/DSB multi-channel systems are 75.9 Gb/s, 62.4 Gb/s and 74.7 Gb/s, respectively. For each transmission system, the corresponding channel bitrate and aggregated transmission capacity are listed in Table 2. Compared with the MF-free SSB multi-channel system, the MF-free DSB multi-channel system has $<18\%$ aggregated signal capacity reductions. This is mainly contributed by the channels located in the 2nd SW channel, where the strong channel fading effect occurs as shown in Fig. 2. However, when the channel fading effect is negligible, both the SSB and DSB bands have similar BER performances and signal transmission capacities, as shown for CH1/CH2 in Fig. 3(b). This agrees well with our theoretical predictions [26]. This suggests that use can be made of SSB (DSB) in the SW channels suffering from the strong (weak) channel fading effect for practical cases, and such design does not considerably reduce the aggregated signal transmission capacity. This is verified by the results in Fig. 3(b), which shows that compared with the MF-free SSB multi-channel systems, the proposed MF-free adaptive SSB/DSB multi-channel system only reduces the aggregated signal transmission capacity by $<1.6\%$. This implies that the proposed technique maintains superiority in enhancing robustness against transmission system impairments/nonlinearity as achieved by the MF-free SSB multi-channel technique. Moreover, such adaptive SSB/DSB variations also reduces the transmitter DSP complexity as discussed in Section 3.4.

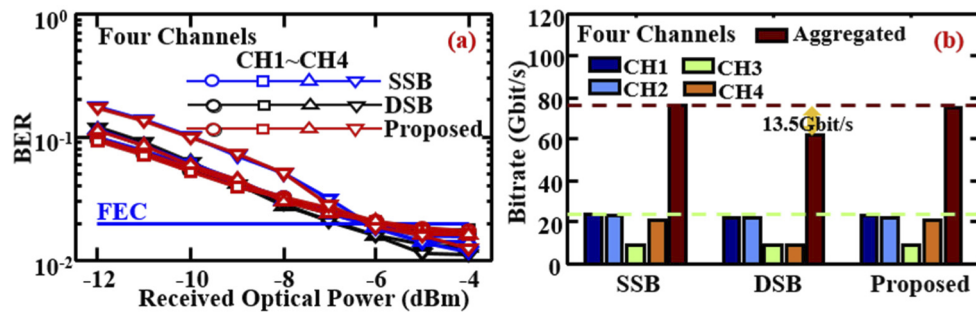


Fig. 3. BER performances (a) and corresponding transmission capacities (b) for Case I, where 4 independent OFDM channels (CH1~CH4) are supported.

3.2. Adaptive reconfiguration of digital filter parameters

When the proposed technique is used in Case I, the impacts of digital filter length variations on the minimum received optical powers of each channel (defined as the receiver sensitivity) for

Table 2. Transmission Capacity (Gbit/s) for Case I

Multi-channel Systems	Channel Bitrate				Aggregated Bitrate
	CH1	CH2	CH3	CH4	
SSB	23.52	22.94	8.82	20.58	75.9
DSB	22.35	22.35	8.82	8.82	62.4
Proposed	22.64	22.35	9.11	20.58	74.7

achieving a BER at the Forward Error Correction (FEC) limit are presented in Fig. 4. Because relatively large digital filter frequency response ripples and power leakage occur for digital filter lengths of < 16 [25], in this section, the digital filter length is selected between 16 and 32. The 1st SW channel operates at DSB, and its conveyed CH1 (CH2) adopts an I-phase (Q-phase) digital filter. For the I/Q-phase digital filter lengths of $L_I=L_Q=16$, compared with CH1, CH2 has a receiver sensitivity degradation of ~ 1 dB due to the Q-phase digital filter's relatively low tolerance to the truncation effect [27]. Prolonging the Q-phase digital filter length L_Q to 32 while still keeping the I-phase digital filter length at $L_I=16$ improves the CH2 receiver sensitivity without affecting CH1's performances. Compared with $L_I=L_Q=32$, $L_I=16/L_Q=32$ give rise to the similar receiver sensitivities and reduce the digital filter DSP complexity by a factor of ~ 1.33 . This result indicates that for the experimental setup, the optimum digital filter lengths are $L_I=16/L_Q=32$. The 2nd SW channel operates at SSB, CH3 and CH4 always have similar BER performances, as shown in Fig. 4. This implies that for SSB signals in a SW channel, the I-phase and/or Q-phase digital filter length variations can simultaneously influence the BER performances of these two SSB signals. In practice, adaptive reconfigurations of digital filter parameters can thus be conducted for each digital filter according to the required signal bitrates. Such adaptive digital filter parameter variation has negligible impacts on digital filter orthogonality, thus offering an effective way of reducing the transmitter digital filter DSP complexity.

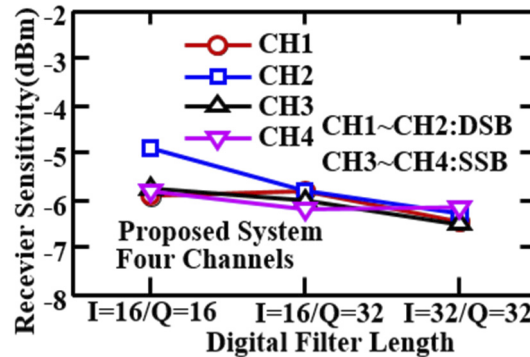


Fig. 4. Receiver sensitivity versus digital filter length performance for Case I, where 4 independent OFDM channels (CH1~CH4) are supported.

3.3. DSP-enabled flexible channel count/bitrate variations, channel bandwidth elasticity and flexible numerology

As explicitly stated in Section 2.1, different up-sampling factors M result in different channel bandwidths, which can subsequently lead to different maximum available channel counts. To explore the DSP-enabled flexibility in channel count/bandwidth variations, in this section, $M1 = 4$ and $M2=M3 = 8$ are used with all other experimental parameters kept similar to those used in obtaining Fig. 3(a). The resulting three SW channels support six independent OFDM channels.

The 1st SW channel has a bandwidth of 10 GHz and conveys two DSB signals. The remaining two SW channels each having a bandwidth of 5 GHz operate at SSB to reduce the channel fading effect. Their channel spectral locations are illustrated in Fig. 2. As seen in Fig. 5(a), by adaptive bit-loading, the BER performances of these OFDM channels are similar to those in Fig. 3(a). The resulting aggregated signal transmission capacity of 72.2 Gb/s is plotted in Fig. 5(b), where the aggregated signal transmission capacity of 74.7 Gb/s for Case I supporting four OFDM channels presented in Fig. 3(b) is also shown. It shows that different up-sampling factors result in variable channel bandwidth/count, which just leads to a <3.5% reduction in aggregated signal transmission capacity due to the channel interferences. For each OFDM channel, the channel bitrate is also variable as a result of bit-loading. It is also worth highlighting that throughout the paper, fixed OFDM signal parameters as listed in the Table 1 are utilized. This means that for the channels employing identical (different) up-sampling factors, they have similar (different) OFDM numerologies. As such, the results in Fig. 5(b) also imply that for the proposed technique, flexible OFDM numerology is achievable by adjusting transmitter DSPs. Due to the digital filtering process, such flexible OFDM numerology variations do not lead to the considerable channel interferences and considerably influence on aggregated transmission capacity.

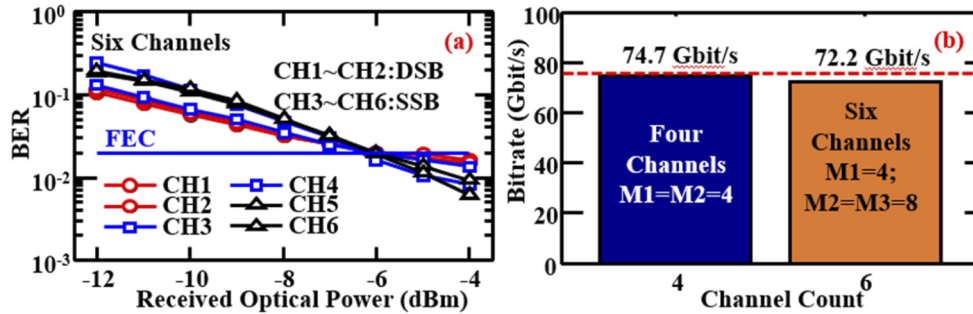


Fig. 5. BER performances (a) and corresponding aggregated transmission capacities (b) for Case II, where 6 independent OFDM channels (CH1~CH6) are supported.

3.4. Transmitter digital filter DSP complexity analysis

Adaptive configuration of digital filter parameters is an effective approach for reducing the transmitter digital filter DSP complexity as discussed in Section 3.2. Following the theoretical analysis of the digital filter DSP complexities of the MF-free SSB and DSB multi-channel techniques and the proposed technique in Section 2.3, in this section, the digital filter DSP complexities of these techniques are calculated utilising the experimental setups/parameters, and the results are presented in Fig. 6, where the identified optimum digital filter lengths of $L_I=16/L_Q=32$ are considered and the up-sampling factors are fixed at 256 for simplicity. For the MF-free SSB (DSB) multi-channel techniques, to support Q SSB (DSB) OFDM channels, the number of the required SSB (DSB) SW channels are assumed to be $\lceil Q/2 \rceil$. Based on the experimental setup, for the considered 20 GHz bandwidth, the power dip caused by the channel fading effects affects the ~ 5 GHz spectral regions. Therefore, in calculating Fig. (6), for the proposed technique, the number of the SSB channels is taken to be $1/4$ of the total number of the channels, and for simplicity, we take $\lceil Q/4 \rceil$. With the SSB and DSB channel counts being made known, the DSP complexity of the proposed technique is calculated utilizing Eq. (5). In obtaining Fig. 6(a), the two OFDM signals in each SW channel have 1000 OFDM symbols are considered, while in Fig. 6(b), the OFDM symbol counts of these two signals in each SW channel are 1000 and 2000. Each OFDM symbol has 34 samples. The results show that when the two signals sharing a SW channel have similar signal lengths, the MF-free SSB and DSB multi-channel

techniques and the proposed technique have similar digital filter DSP complexities. While when the two signals sharing a SW channel have different signal lengths, the proposed technique has a digital filter DSP complexity similar to the MF-free DSB multi-channel techniques, which are lower than the MF-free SSB multi-channel techniques. This agrees very well with the theoretical analysis in Section 2.3. This implies that the proposed technique is suitable for applications requiring multiple dynamic connections in a large diversity of traffic loading environment.

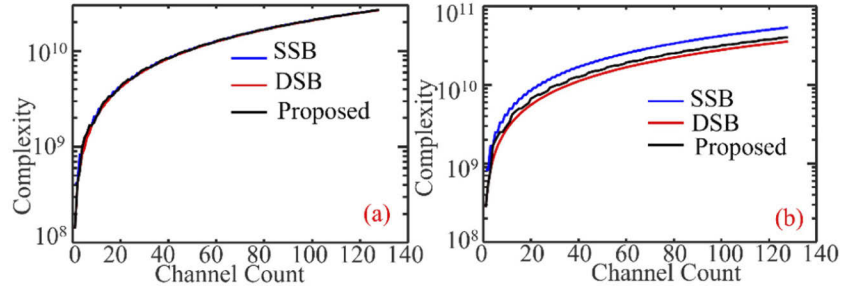


Fig. 6. Digital filter DSP complexity as a function of channel count. (a) an identical signal length assumed for two signals in each SW channel, (b) different signal lengths assumed for two signals in each SW channel

For a given IMDD system with a fixed total bandwidth and transmission distance, the spectral region strongly affected by the channel fading effect is independent of overall channel count. All the channels located in this region may operate at SSB for achieving high spectral efficiency. As such, increasing the overall channel count may not effectively decrease the number of channels affected by the channel fading effect. In addition, for practical applications, the maximum channel count is determined mainly by the finite logical resources associated with FPGAs/ASICs implemented in corresponding transceivers. For a given FPGA/ASIC, multiple parallel FPGAs/ASICs may be employed to further increase the channel count.

It is worth mentioning the following four aspects of the proposed technique: 1) the proposed system still maintains a relatively low receiver DSP complexity due to the exclusion of MFs [23,26]; 2) all the above salient features of the proposed technique are achievable using DSPs without performing any modifications to network architectures; 3) similar to the MF-free SSB multi-channel technique, the proposed technique fully supports concurrent direct end-user communications [25] to greatly reduce the fibre propagation delay and to enhance the aggregated transmission capacity; 4) OFDM subcarrier I/Q data and bit data can be obtained respectively after the sideband processing operation and decoding operation in the receiver DSPs. Thus, this technique has excellent compatibility with flexible low layer functional splits, this has sufficient potential for practical implementations in 5G and beyond networks.

4. Conclusions

A MF-free adaptive SSB/DSB multi-channel technique with excellent DSP-enabled adaptability, flexibility and elasticity has been proposed and experimentally demonstrated in a $>72\text{Gb/s}@25\text{ km}$ IMDD transmission system. The DSP-enabled flexibility, adaptability and elasticity improvements have been experimentally assessed, and its robustness against transmission system impairment/nonlinearity has been compared with the previously reported MF-free SSB and DSB multi-channel techniques. Comprehensive digital filter DSP complexity analyses have been made for these MF-free orthogonal digital filtering-enabled multi-channel aggregation techniques. It has been shown that the proposed technique maintains the MF-free SSB multi-channel technique's excellent robustness to transmission system impairments/nonlinearity with just $<1.6\%$ reductions

in aggregated signal transmission capacity. Without requiring extra electrical and optical components and modifying network architectures, flexible channel count/bitrate and OFDM numerology variations and elastic bandwidth provision are achievable via transmitter DSP functions, which only cause <3.5% aggregated transmission capacity reductions. In addition, a transceiver with low DSP complexity is feasible by adaptively reconfiguring digital filter parameters and selecting SSB and DSB. This work demonstrates that the technical feasibility of utilizing digital orthogonal filtering to implement flexible, elastic and adaptive networks for 5G and beyond.

Funding. DESTINI project funded by the ERDF under the SMARTEexpertise scheme; DSP Centre funded by the ERDF through the Welsh Government.

Disclosures. The authors declare no conflicts of interest.

Data availability. Data underlying the results presented in this paper are not publicly available at this time but may be obtained from the authors upon reasonable request.

References

1. P. T. Dat, A. Kanno, N. Yamamoto, and T. Kawanishi, "Seamless convergence of fiber and wireless systems for 5G and beyond networks," *J. Lightwave Technol.* **37**(2), 592–605 (2019).
2. A. O. Mufutau, F. P. Guiomar, M. A. Fernandes, A. Lorences-Riesgo, A. Oliveira, and P. P. Monteiro, "Demonstration of a hybrid optical fiber–wireless 5G fronthaul coexisting with end-to-end 4G networks," *J. Opt. Commun. Netw.* **12**(3), 72–78 (2020).
3. H. Zeng, X. Liu, S. Megeed, N. Chand, and F. Effenberger, "Real-time demonstration of CPRI-compatible efficient mobile fronthaul using FPGA," *J. Lightwave Technol.* **35**(6), 1241–1247 (2017).
4. 3GPP, "Study on new radio access technology: Radio access architecture and interfaces," Sophia Antipolis, France, Rep. TR 38.801, 2017.
5. L. M. P. Larsen, A. Checko, and H. L. Christiansen, "A survey of the functional splits proposed for 5G mobile crosshaul networks," *IEEE Commun. Surv. Tut.* **21**(1), 146–172 (2019).
6. I. A. Alimi, A. L. Teixeira, and P. P. Monteiro, "Toward an efficient C-RAN optical fronthaul for the future networks: a tutorial on technologies, requirements, challenges, and solutions," *IEEE Commun. Surv. Tut.* **20**(1), 708–769 (2018).
7. M. Ruffini, "Multidimensional convergence in future 5G networks," *J. Lightwave Technol.* **35**(3), 535–549 (2017).
8. L. Li, M. Bi, H. Xin, Y. Zhang, Y. Fu, X. Miao, A. M. Mikaeil, and W. Hu, "Enabling flexible link capacity for eCPRI-based fronthaul with load-adaptive quantization resolution," *IEEE Access* **7**, 102174–102185 (2019).
9. eCPRI Specification V1.1.1. Interface Specification, Common Public Radio Interface, Jan. 2018.
10. D. Wake, A. Nkansah, and N. J. Gomes, "Radio over fiber link design for next generation wireless systems," *J. Lightwave Technol.* **28**(16), 2456–2464 (2010).
11. S. Cho, H. Park, H. S. Chung, K. H. Doo, S. Lee, and J. H. Lee, "Cost-effective next generation mobile fronthaul architecture with multi-IF carrier transmission scheme," *Proc. Opt. Fiber Commun.* San Francisco, CA, USA, Tu2B.6 (2014).
12. P. Torres-Ferrera, S. Straullu, S. Abrate, and R. Gaudino, "Upstream and downstream analysis of an optical fronthaul system based on DSP-Assisted channel aggregation," *J. Opt. Commun. Netw.* **9**(12), 1191–1201 (2017).
13. X. Liu, H. Zeng, N. Chand, and F. Effenberger, "Efficient mobile fronthaul via DSP-based channel aggregation," *J. Lightwave Technol.* **34**(6), 1556–1564 (2016).
14. H. Li, Q. Yang, S. Fu, M. Luo, X. Li, Z. He, P. Jiang, Y. Liu, and S. Yu, "Digital code-division multiplexing channel aggregation for mobile fronthaul architecture with low complexity," *IEEE Photon. J.* **10**(2), 1–10 (2018).
15. M. Sung, S. Cho, H. S. Chung, S. M. Kim, and J. H. Lee, "Investigation of transmission performance in multi-IFoF based mobile fronthaul with dispersion-induced intermixing noise mitigation," *Opt. Express* **25**(8), 9346–9357 (2017).
16. S. Noor, P. Assimakopoulos, M. Wang, H. A. Abdulsada, N. Genay, L. A. Neto, P. Chancelou, and N. J. Gomes, "Comparison of digital signal processing approaches for subcarrier multiplexed 5G and beyond analog fronthaul," *J. Opt. Commun. Netw.* **12**(3), 62–71 (2020).
17. M. Bolea, R. P. Giddings, M. Bouich, C. Aupetit-Berthelemot, and J. M. Tang, "Digital filter multiple access PONs with DSP-enabled software reconfigurability," *J. Opt. Commun. Netw.* **7**(4), 215–222 (2015).
18. X. Duan, R. P. Giddings, S. Mansoor, and J. M. Tang, "Experimental demonstration of upstream transmission in digital filter multiple access PONs with real-time reconfigurable optical network units," *J. Opt. Commun. Netw.* **9**(1), 45–52 (2017).
19. M. L. Deng, T. Mamadou, Z. B. Xing, X. Kang, Z. R. Luo, J. W. Shi, and L. Wang, "Digital orthogonal filtering-enabled synchronous transmissions of I/Q waveforms and control words for bandwidth-efficient and low-complexity mobile fronthaul," *Opt. Fiber Commun. Conf., F1D.2*, USA, 2021.
20. P. Assimakopoulos, S. Noor, M. Wang, H. Abdulsada, L. A. Neto, N. Genay, P. Chancelou, and N. J. Gomes, "Flexible and efficient DSP-assisted subcarrier multiplexing for an analog mobile fronthaul," *IEEE Photon. Technol. Lett.* **33**(5), 267–270 (2021).

21. E. Al-Rawachy, R. P. Giddings, and J. M. Tang, "Experimental demonstration of a DSP-based cross-channel interference cancellation technique for application in digital filter multiple access PONs," *Opt. Express* **25**(4), 3850–3862 (2017).
22. E. Al-Rawachy, R. P. Giddings, and J. M. Tang, "Experimental demonstration of a real-time digital filter multiple access PON with low complexity DSP-based interference cancellation," *J. Lightwave Technol.* **37**(17), 4315–4329 (2019).
23. W. Jin, A. Sankoh, Y. X. Dong, Z. Q. Zhong, R. P. Giddings, M. O'Sullivan, J. Lee, T. Durrant, and J. M. Tang, "Hybrid SSB OFDM-digital filter multiple access PONs," *J. Lightwave Technol.* **38**(8), 2095–2105 (2020).
24. Z. Q. Zhong, W. Jin, Y. X. Dong, A. Sankoh, J. X. He, Y. H. Hong, R. P. Giddings, I. Pierce, M. O'sullivan, J. Lee, G. Mariani, T. Durrant, and J. M. Tang, "Experimental demonstrations of matching filter-free digital filter multiplexed SSB OFDM IMDD transmission systems," *IEEE Photon. J.* **13**(2), 7900512 (2021).
25. Z. Zhong, W. Jin, S. Jiang, J. He, D. Chang, R. Giddings, Y. Hong, M. O'Sullivan, T. Durrant, G. Mariani, J. Trewern, and J. Tang, "Experimental demonstrations of concurrent adaptive inter-ONU and upstream communications in IMDD hybrid SSB OFDM-DFMA PONs," *Proc. Opt. Fiber Commun. Conf.*, USA, F4I.5 (2021).
26. A. Sankoh, W. Jin, Z. Zhong, J. He, Y. Hong, R. P. Giddings, I. Pierce, M. O'Sullivan, J. Lee, T. Durrant, and J. Tang, "Hybrid OFDM-digital filter multiple access PONs utilizing spectrally overlapped digital orthogonal filtering," *IEEE Photon. J.* **12**(5), 1–11 (2020).
27. X. Duan, R. P. Giddings, M. Bolea, Y. Ling, B. Cao, S. Mansoor, and J. M. Tang, "Real-time experimental demonstrations of software reconfigurable optical OFDM transceivers utilizing DSP-based digital orthogonal filters for SDN PONs," *Opt. Express* **22**(16), 19674–19685 (2014).
28. 3GPP, "Study on New Radio (NR) access technology," Sophia Antipolis, France, Rep. TR 138 912, 2018.